Coordination Chemistry Reviews 254 (2010) 273–287

Contents lists available at ScienceDirect

Coordination Chemistry Reviews

journal homepage: www.elsevier.com/locate/ccr

Review

Mechanistic analysis of the transition metal-catalyzed hydrogenation of imines and functionalized enamines

Amandine Fabrello[a,b], Alice Bachelier[a,b], Martine Urrutigoïty[a,b,*], Philippe Kalck[a,b,*]

[a] CNRS, LCC UPR 8241 (Laboratoire de Chimie de Coordination), 205 route de Narbonne, F-31077 Toulouse, France
[b] Université de Toulouse, UPS, INPT, LCC, F-31077 Toulouse, France

Contents

ARTICLE INFO

Article history:
Received 13 March 2009
Accepted 3 September 2009
Available online 9 September 2009

Keywords:
Homogeneous catalysis
Metal-catalyzed hydrogenation
Hydrogenation mechanism
Chiral ligands
Rhodium catalysts
Iridium catalysts
Asymmetric induction
Ruthenium Shvo's catalyst

ABSTRACT

The asymmetric hydrogenation of prochiral imines has been mainly studied on cationic rhodium or iridium complexes and involves the coordination of the nitrogen atom on the metal centre. Oxidative addition of dihydrogen followed by one hydride transfer onto the carbon atom produces a σ-bonded nitrogen-metal intermediate from which reductive elimination occurs with the second hydride to produce the amine. From all these reactivity studies we propose that in an early step a hydrogen atom transfer could occur on the nitrogen atom to generate an iminium species which coordinates the metal centre through the C=N double bond. The Shvo catalyst, an active neutral ruthenium(II) complex, presents the particularity to transfer almost simultaneously a proton from the hydroxycyclopentadienyl ligand and a hydride bonded to the metal center. In this case too, we suggest the first proton transfer generates an iminium species.

Morever, a few titanium complexes have been shown to catalyze the hydrogenation of imines.

Concerning enamines, literature is rather scarce on catalytic success. On the contrary, many studies focused on hydrogenation of enamides, which represent functionalized enamines, and enantiomeric excesses very close to 100% have been obtained. Extensive studies of the effect of the (chiraldiphosphine)Rh^+ framework on the asymmetric induction have shown that several reversible steps can occur related to the oxidative addition of dihydrogen before or after the coordination of the enamide; the irreversible step directly connected to the asymmetric induction is the formation of the chiral alkyl-rhodium species.

1. Introduction

Asymmetric catalysis represents an elegant way to directly produce chiral compounds by functionalization of a prochiral substrate. Many catalytic reactions have proven to be efficient, in particular the hydrogenation of alkenes or ketones, and enantioselectivities resulting in enantiomeric excess (e.e.) values near to 100% have been reached [1,2]. During the past decades numerous chiral ligands have been designed and synthesized so that transition metal/chiral ligand pairs can be found to transform selectively a given substrate combining high rates and chemo- as well as regioselectivities. Most of the ligands contain two donating phosphorus atoms coordinated to late transition metals. Generally, in these complexes, the chiral information arises either from

* Corresponding authors at: ENSIACET, 118 route de Narbonne, 31077 Toulouse Cedex 4, France. Tel.: +33 562 885698/690; fax: +33 562 885600.
E-mail addresses: martine.urrutigoity@ensiacet.fr (M. Urrutigoïty), philippe.kalck@ensiacet.fr (P. Kalck).

0010-8545/$ – see front matter © 2009 Published by Elsevier B.V.
doi:10.1016/j.ccr.2009.09.002

stereogenic phosphorus atoms or the carbon backbone, or from atropoisomerism as well as planar chirality [3–7]. More recently, mixed ligands containing phosphorus and nitrogen atoms and monodentate ligands [8,9], including carbenes [10], have also proven to be efficient.

Chiral amines represent an important class of molecules in fine chemistry since they are useful building blocks to synthesize agrochemical and pharmaceutical active products. However, asymmetric hydrogenation of imine and enamine functionalities remains a significant challenge as far as activity and enantioselectivity are concerned [11]. Prochiral imines and protected enamines such as enamides can be now efficiently hydrogenated [12], but the direct transformation of an enamine is only illustrated in a few recent reports [13–16]. Attractive results have been reported by the research groups of Andersson [14], Zhou [15], and Pfaltz [16] on enamines using new generations of chiral P-N ligands or spirophosphonites. N-acyl groups or oxygen-containing substituents in α- or β-position on the enamine substrate appear to play a prominent role in forming a chelating ligand on the metal center, and inducing good reactivity associated to high e.e. values [17–19].

In order to have a complete insight into the synthesis of chiral amines by asymmetric hydrogenation of unsaturated substrates, it appears crucial to possess the mechanistic knowledge of the full catalytic cycle. More especially it is important to understand how the substrate coordinates the metal center and how the hydrogen atoms are transferred to either the C=N unsaturation for imines, or the C=C bonds for enamines This review is devoted to the studies conducted on the reactivity of prochiral imines, enamines and extended to amides because they represent a protected and activated form of this latter substrate leading to enhanced activities. We will particularly focus our analysis on the mechanisms by which theses substrates undergo selective and more particularly enantioselective reduction.

2. Imines

The first hydrogenation of a prochiral imine dates from 1975 when a Rh/(DIOP) complex was shown to hydrogenate slowly Ph-C(Me)=NCH$_2$Ph with a 20% e.e. [20,21]. Ten years later, improvements were modest since the e.e. values reached only 60–70%. Many efforts have been done to improve the enantiomeric excess as well as the catalytic performance, i.e. not only the turnover number but also the turnover frequency. The most recent reports show that, either by hydrogenation with dihydrogen or through hydrogen transfer from an alcohol or an organic acid (in this case for the iminium salt and not for imine), this goal can be achieved [22,23].

We will focus our attention on recent papers that explore and provide deeper insight into the hydrogenation mechanisms of various types of imines.

2.1. Mechanism of the H_2 hydrogenation of imines

Recent studies have been devoted to the reactivity of cationic iridium or rhodium complexes in the hydrogenation of imines, giving insight into the mechanism of the reaction. These reports by James [24–33], Bianchini [34,35], Oro [36–39] and their research teams, show that a dihydrido complex containing the imine coordinated via the nitrogen atom plays a key role in the catalytic cycle. Bianchini et al. reported the reaction of $[Ir(\mu\text{–}Cl)(\eta^4\text{–}C_8H_{12})]_2$ with the $P(CH_2Ph)_3$ ligand affording $[IrCl(\eta^4\text{–}C_8H_{12})\{P(CH_2Ph)_3\}]$, followed by addition of pyridine and $[NH_4][PF_6]$ in methanol leading to the salt $[Ir(\eta^4\text{–}C_8H_{12})(NC_5H_5)\{P(CH_2Ph)_3\}][PF_6]$ **1**. The cation readily reacts with dihydrogen in a coordinating solvent such as THF to provide the dihydride $[Ir(H)_2(THF)_2(NC_5H_5)\{P(CH_2Ph)_3\}]^+$ **2**. The two hydride ligands are in mutual *cis*-position, two coordinated solvent (THF) molecules are present, the cyclooctadiene ligand being first hydrogenated and removed as cyclooctane. In situ NMR experiments show that addition of the imine N-(β-naphthylmethylene)aniline (NpCH=NPh) substitutes progressively the two THF molecules, providing at first $[Ir(H)_2(THF)(NpCH{=}NPh)(NC_5H_5)\{P(CH_2Ph)_3\}]^+$ **3**, and then $[Ir(H)_2(NpCH{=}NPh)_2(NC_5H_5)\{P(CH_2Ph)_3\}]^+$ **4** in the presence of an excess of imine. As shown by kinetic studies, a reversible transfer of the two hydrides takes place to produce an iridium(I) intermediate containing all the four pyridine, phosphine, imine and amine ligands, i.e. $[Ir(NpCH{=}NPh)(NpCH_2\text{-}NHPh)(NC_5H_5)\{P(CH_2Ph)_3\}]^+$ **5**. The oxidative addition of dihydrogen, followed by release of the amine and coordination of THF, can be considered as the rate determining step which restores complex **3** (Scheme 1).

The question arises about the intimate mechanism of the hydride transfer in **4** to produce species **5**. The imine molecule

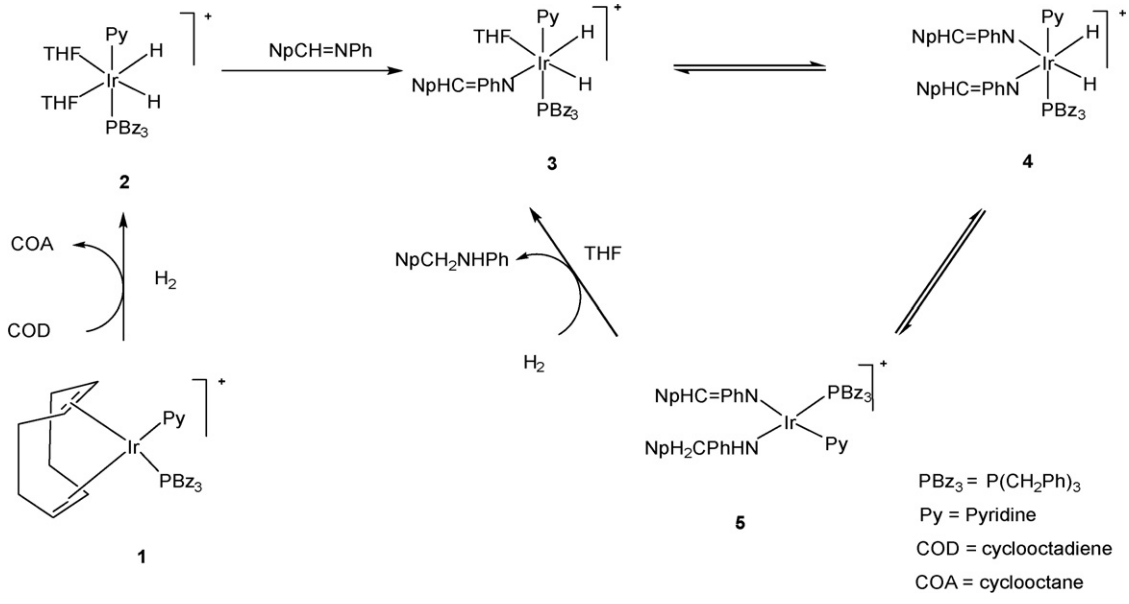

Scheme 1. Catalytic cycle from the precursor $[Ir(\eta^4\text{-}C_8H_{12})(NC_5H_5)\{P(CH_2Ph)_3\}][PF_6]$, adapted from Ref. [35].

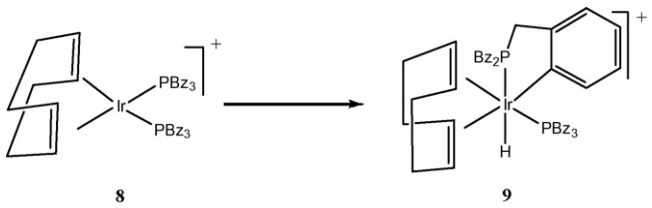

Scheme 2. Equilibrium between $[(\eta^4\text{-}C_8H_{12})Ir(PBz_3)_2]^+$ **8** and the corresponding ortho-metallated complex **9**, adapted from Ref. [35].

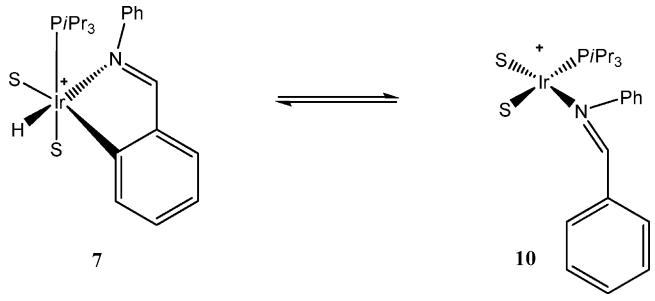

Scheme 3. Equilibrium between **7** and **10**.

might be coordinated to the metal center either through the lone pair of the nitrogen atom or by the C=N double bond in a η^2-mode. It is important to mention at this point the intermediate complex characterized by Oro et al. [36,37], after reaction of benzylideneaniline (PhN=CHPh) with the solvated complex $[Ir(H)_2(CH_3CN)_3\{P(iPr)_3\}][BF_4]$ **6** which affords $[Ir(H)\{PhN{=}CH(C_6H_4)\text{-}\kappa^2N,C\}(CH_3CN)_2\{P(iPr)_3\}][BF_4]$ **7**. In this complex the imine is coordinated through the lone pair of the nitrogen atom and an orthometallation has occurred on the phenyl substituent. A similar stabilization by orthometallation reported by Bianchini and al. [35] occurs in the complex $[(\eta^4\text{-}C_8H_{12})Ir(PBz_3)_2]^+$ **8**. In $CHCl_3$, at room temperature, it generates spontaneously the hexacoordinated iridium(III) species **9** (Scheme 2) with the two phosphine ligands in *cis*-position.

If we consider the two observations, we can conclude that an imine approaches the iridium centre by the nitrogen atom and that the active species should be the square planar species **10** (Scheme 3) on which oxidative addition of H_2 can occur.

Thus, from all these studies, we suggest (Scheme 4) that the mechanism could consist in an intramolecular nucleophilic attack of a hydride ligand onto the imine carbon atom, either involving **4** or **4′** (for the η^2-mode). From the intermediate species **4‡**, reductive elimination could occur to give the amine $HN(Ph)CH_2Np$ coordinated to give the iridium(I) complex **5**.

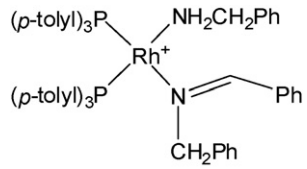

Scheme 5. Representation of complex **11**, adapted from Ref. [27].

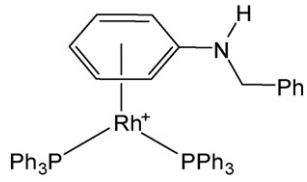

Scheme 6. Complex **12**, adapted from Ref. [24].

Moreover, James and coworkers isolated the cationic rhodium(I) complex **11** in which the imine is N-coordinated [27]. The coordination sphere is completed by two tris(p-tolyl)phosphine ligands and by benzylamine arised from the hydrolysis of the imine (Scheme 5).

Previous studies by the same research group showed that the inhibiting effect produced by the amine after hydrogenation of the imine catalyzed by $[Rh(MeOH)_2(PPh_3)_2]^+$ does result from the coordination of the amine [24]. In fact, the X-ray crystal structure shows that coordination occurs through the phenyl ring of phenylbenzylamine, as represented for **12** (Scheme 6).

By NMR spectroscopy the authors detected two isomers for complex **12** before it dissociates amine. The first isomer possesses the structure shown in Scheme 6, whereas the geometry of the second one is unclear and from the spectroscopic data the authors propose that the $[Rh(PPh_3)_2]$ moiety coordinates the ionized form of the amine, i.e., that one shown in Scheme 7. Thus such a coordination mode would involve an iminium cation.

This coordination was evidenced in the case of an iridium complex by an X-ray crystal structure determination, showing that the phenyl ring is η^5-bonded to the iridium center as shown for **13**, an 18e complex (Scheme 8) [38].

This schematic representation is consistent with the five Ir–C bond lengths which present the same order of magnitude, the sixth carbon atom (C=N double bond) being not coordinated. At low

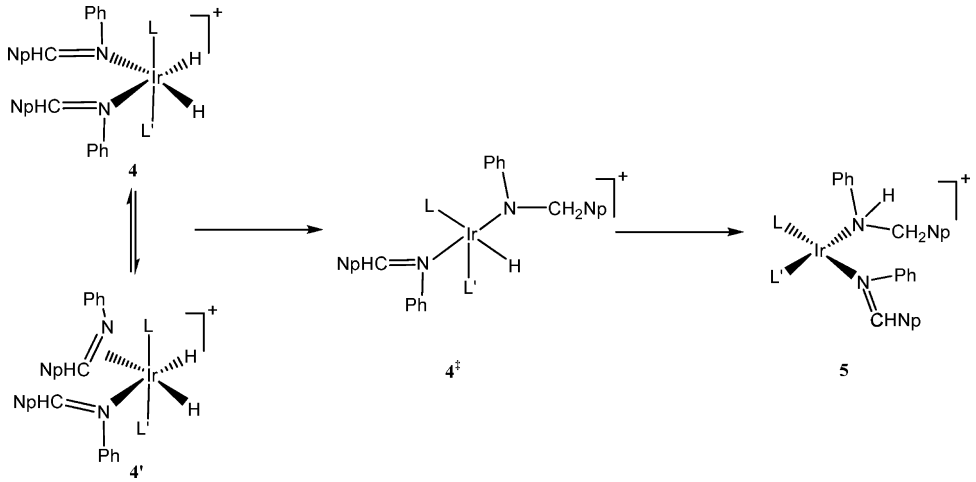

Scheme 4. Mechanism leading from **4** or **4′** to **5** through **4‡**.

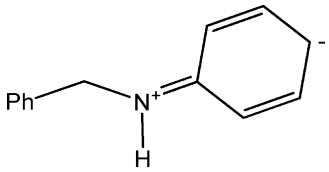

Scheme 7. Ionic form of phenylbenzylamine, adapted from Ref. [24].

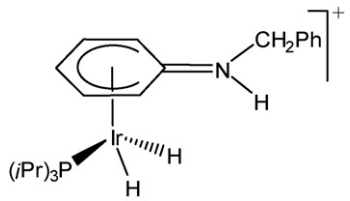

Scheme 8. Complex **13**, adapted from Ref. [38].

amine concentration this ligand can be displaced by the solvent and a fortiori by the imine, which undergoes orthometallation. Species **13** was recognized as the resting state by reactivity studies; Oro et al. observed two Ir–H signals at ca. −17 ppm for this complex, clearly pointing their hydridic character. The mechanism they suggested supposes the interaction of an extra amine molecule with **13** (complex **14**), based on NMR studies, deuteriation experiments and DFT calculations. They consider a further intermediate (complex **15**) in which one hydride ligand has been transferred from the iridium center and H_2 oxidative addition has occurred. This mechanism is shown in Scheme 9.

Thus in the η^5-coordinated amine in **13**, the approach of the amine shifts the phenyl coordination in a η^6-mode to give **14**. In this latter species the incoming amine interacts through hydrogen bonds both with one hydride ligand and the nitrogen atom of the coordinated amine. In **15**, after the oxidative addition of H_2, the incoming amine has been transformed in an ammonium species hydrogen-bonded to the coordinated amine. Then, this hydrogen atom is transferred to the η^4-C_6H_5-coordinated amine to provide a η^4-C_6H_5-ammonium ligand. The approach of an imine ligand substitutes the amine ligand and provides **16** (Scheme 10).

Formally, simultaneous transfer of a proton from the η^4-C_6H_5-ammonium ligand and a hydride from the iridium center can occur. Another mechanistic pathway could be proposed in which the first proton transfer produces the iminium substrate coordinating iridium through the C=N double bond, complex **17** as shown in Scheme 11. Then, an intramolecular nucleophilic attack of a hydride ligand on the carbon atom gives σ-bonded Ir–N ammonium species from which decoordination leads to the NHPh(CH_2Ph) amine and the cationic iridium dihydride.

The hydrogenation of imines has been also achieved by the use of a dinuclear iridium cationic precursor [39]. It results from the protonation by HBF_4 of the neutral tetrahydride complex [Ir_2(μ-H)(μ-pyrazol)$_2$(H)$_3$(CH_3CN){P(iPr)$_3$}$_2$] **18** (pyrazol = $N_2C_3H_3$ or pz), giving the formula [Ir_2(μ-H)(μ-pz)$_2$(H)$_2$(η^2-H_2)(CH_3CN){P(iPr$_3$}$_2$]$^+$ **19**. Aryl- or alkylimines are easily protonated by **19** even at low temperatures, and restore complex **18**. This latter complex hydrogenates the resulting iminium molecule affording [Ir_2(μ-H)(μ-pz)$_2$(H)$_2$(CH_3CN){κ^1-NHPh(CH_2Ph)}(PiPr$_3$)$_2$]$^+$ **20**. From the isolation and characterization of these complexes, the authors proposed the simplified catalytic cycle shown in Scheme 12 [39].

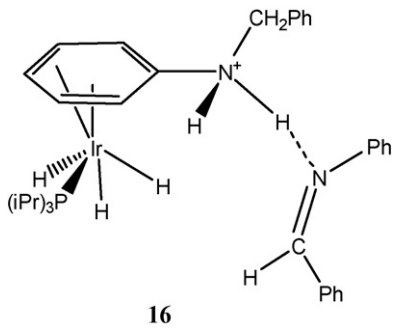

16

Scheme 10. Complex **16**.

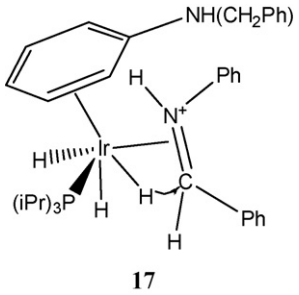

17

Scheme 11. Complex **17**.

An alternative pathway could be to substitute the imine substrate to the amine ligand in complex **20** to produce the cationic complex **21**. Then hydride transfer generates the η^2-coordinated iminium species **22**.

Coordination of H_2 followed by its oxidative addition provides the intermediate **23**. The hydride transfer provides species **20** and the last step does in fact involve the amine substitution for the imine.

In addition, Oro et al. have studied the reactivity of the neutral triflate species **24** [Ir_2(μ-H)(μ-pz)$_2$(H)$_2$(CH_3CN){κ-OSO_2CF_3}{P(iPr)$_3$}$_2$] [39]. They have substituted acetonitrile with L=CO, η^2-C_2H_4 or pyridine and evidenced on the catalytic hydrogenation rates a strong influence of the L ligand in trans-position to the bridging hydride.

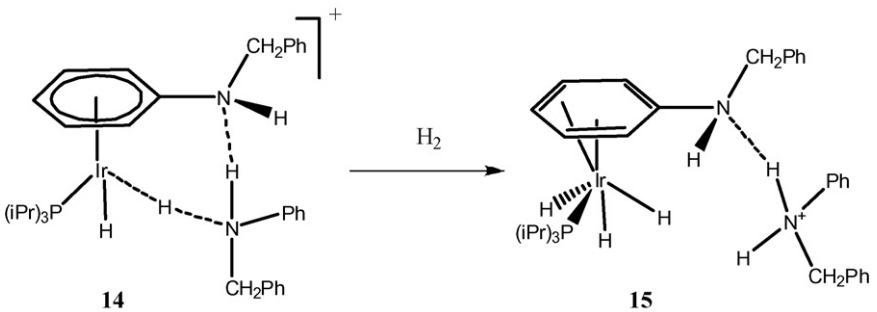

14 **15**

Scheme 9. Representation of complexes **14** and **15**.

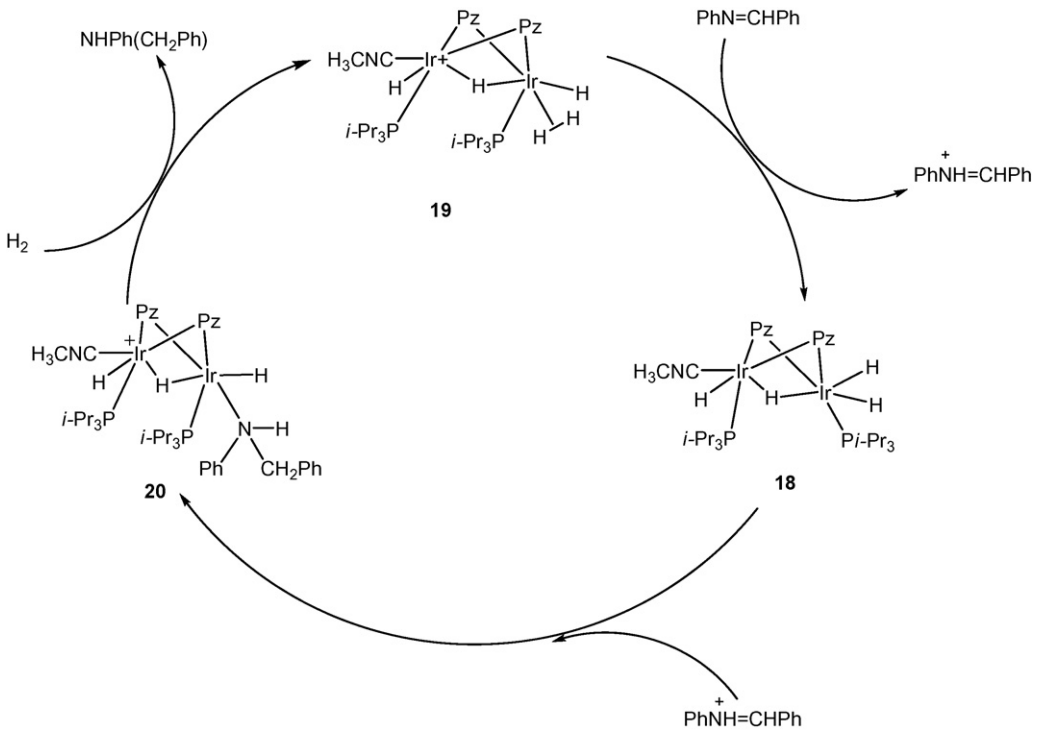

Scheme 12. Catalytic cycle adapted from Ref. [39].

From kinetic measurements and NMR observations, Bianchini and co-workers have proposed that the complex $[Ir(H)_2(NpCH{=}NPh)_2\{P(CH_2Ph)_3\}_2]^+$ **25** undergoes intramolecular hydride transfer to give the iridium(I) intermediate $[Ir(NpCH{=}NPh)(NpCH_2NHPh)\{P(CH_2Ph)_3\}_2]^+$ **26** containing both coordinated the imine and the corresponding amine [35]. The rate-determining step is the activation of dihydrogen by **26**, producing $[Ir(H)_2(NpCH{=}NPh)(NpCH_2NHPh)\{P(CH_2Ph)_3\}_2]^+$ **27**. In this case too the incoming imine substitutes the coordinated amine, thus restoring complex **25**. As we have done previously (Schemes 13 and 14), we propose a two step hydride transfer from **25** to **26**, as shown in Scheme 15.

The first hydride transfer should occur on the coordinated nitrogen atom. The resulting intermediate **25a** shows the iminium molecule coordinated in a η^2-mode, and the second hydride transfer provides **26**. In this catalytic cycle the rate determining step

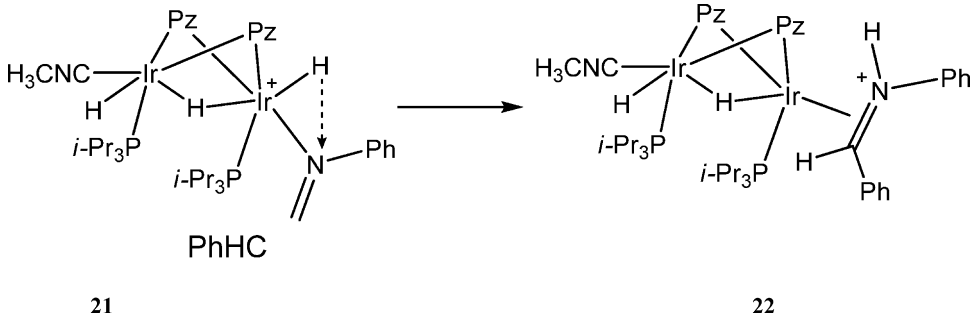

Scheme 13. Hydrogen atom transfer in species **21** to produce **22**.

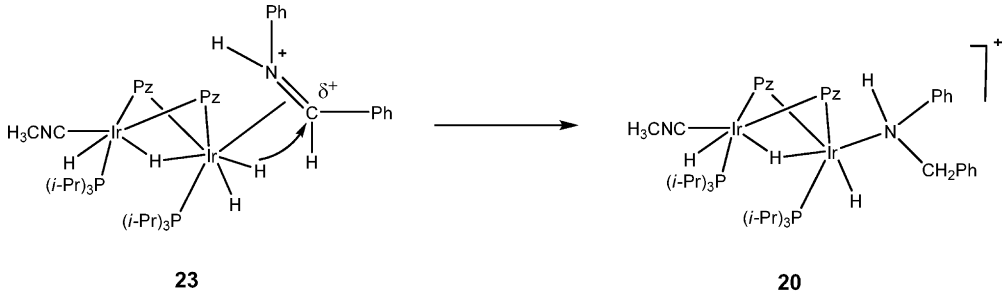

Scheme 14. Hydride transfer to iminium intermediate **23**.

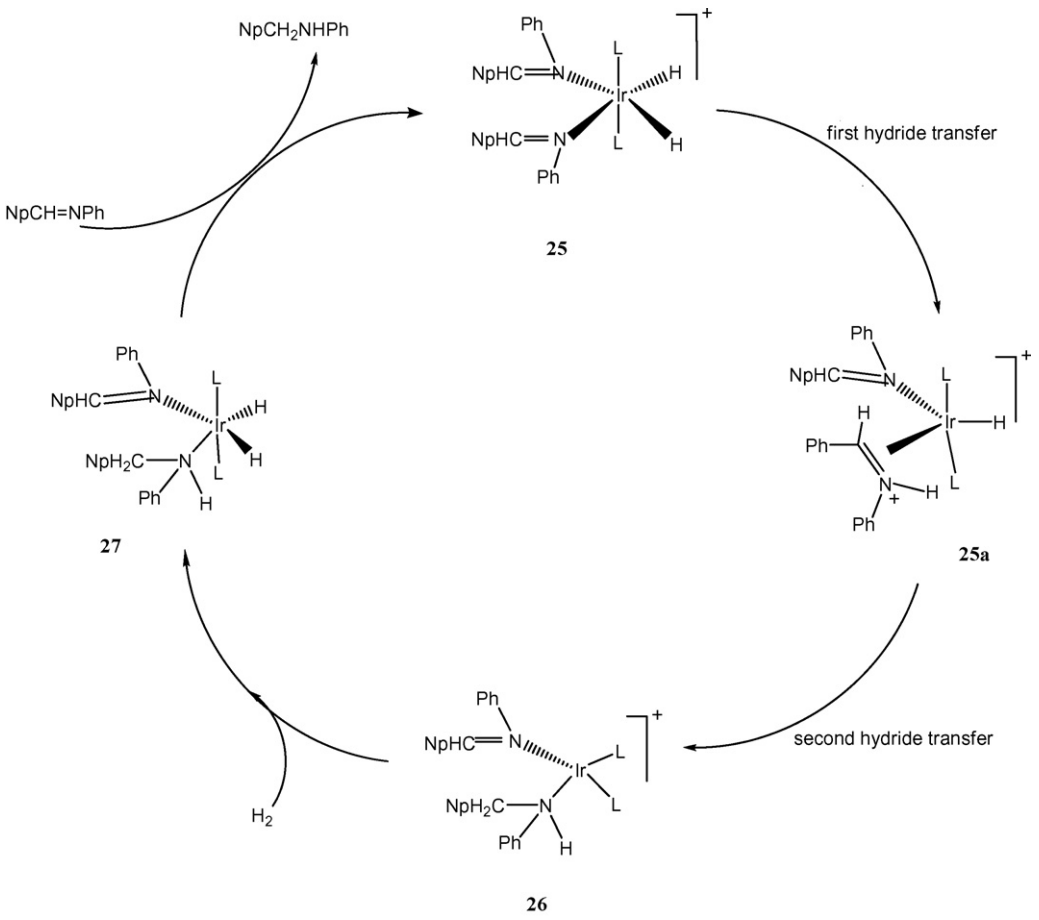

Scheme 15. Catalytic cycle adapted from Ref. [35], **25a** has been added and L=$P(CH_2Ph)_3$.

concerns the oxidative addition of dihydrogen to provide **27**. Then, a fast replacement of the amine by an imine molecule restores the active species **25**.

In conclusion, from all the previous mechanistic approaches, we can propose that the intimate hydrogenation mechanism involves the key short-lived intermediate **A** containing a hydride ligand and the η^2-iminium ligand as schematically displayed in Scheme 16.

This proposal is supported by the observation of Oro et al. who showed that the t-butyl imine ^{t}BuN=CHPh can also be hydrogenated [39]. At low temperature (−78 °C), this imine reacts with complex **19** to deprotonate it, producing the neutral species **18** and the iminium cation [^{t}BuNH=CHPh]$^+$. At −20 °C this cation interacts with **18** to give **20**, containing the coordinated ^{t}BuNHCH$_2$Ph amine ligand.

It is worth noting that coordination of phenyl ring as in **13** or orthometallation as observed in **7** or **9** can presumably afford stable species, representative of the relevant resting states. According to the nature of the imine ligands, the relative reaction rates of the various catalytic steps can notably differ. However, the key species appears to be the intermediate **A** in which the [M]−H ligand reacts very quickly to produce the expected amine.

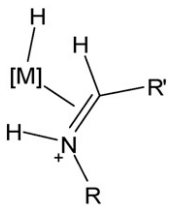

Scheme 16. Key intermediate **A**.

Thus, the active species is a rhodium or an iridium cationic complex in which the metal center is coordinated by two phosphine ligands, the imine and, according to the electron density, either a solvent molecule or a strong amine resulting either from the imine hydrogenation or eventually the imine hydrolysis. The key step is the oxidative addition of dihydrogen to this **B** intermediate to produce the dihydride complex **C** (Scheme 17). The first hydrogen atom transfer occurs on the nitrogen atom of the imine which results in the formation of the η^2-iminium intermediate **A**, the cationic charge being localized on the nitrogen atom. The second hydrogen atom transfer is an intrasphere nucleophilic attack on the carbon atom of the N^+=C double bond resulting in the pentacoordinated Rh(I) or Ir(I) complex **D**. The last step of this catalytic cycle is the release of the expected amine and the coordination of the incoming imine to produce again **B.** If the reaction rates of the four main steps are not very high, side-complexes which are most often in equilibrium with **B**, **C**, or **D**, can appear with the coordination of an arene ring (η^4 or η^6-mode) or with an orthometallation of a side phenyl group.

2.2. Mechanism of the ruthenium H_2 hydrogenation of imines

In 1985 Shvo reported a dinuclear ruthenium hydride complex, which can hydrogenate alkenes, aldehydes and ketones under rather mild conditions (33 bar, 145 °C) with good turnover frequencies [40,41]. The X-ray crystal structure of this precursor was solved

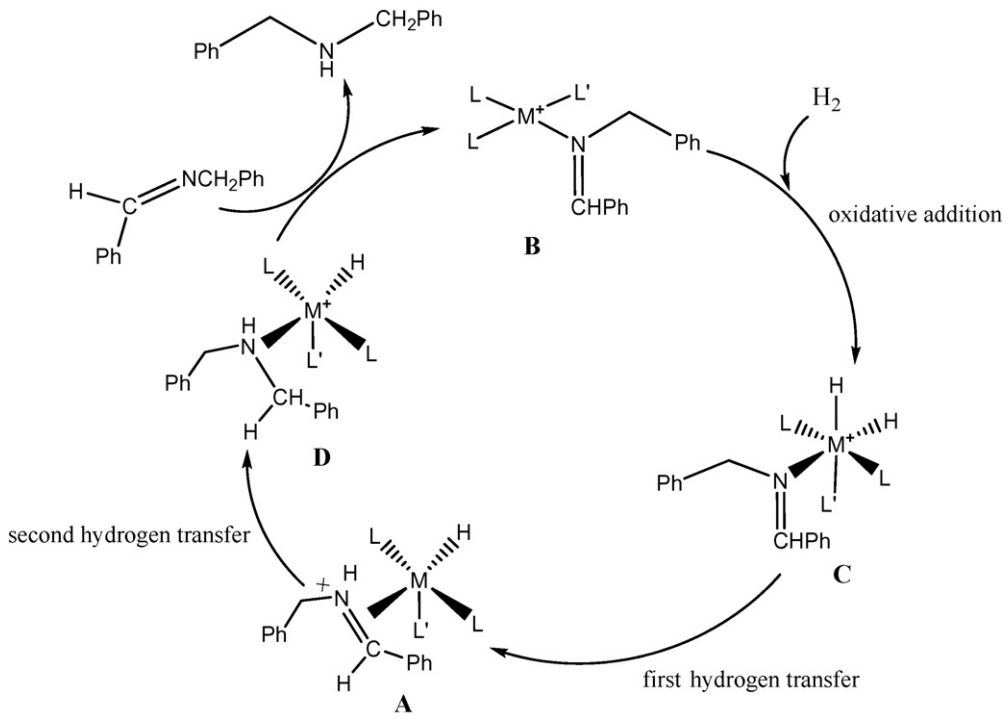

Scheme 17. General catalytic cycle showing the main intermediates during rhodium- or iridium-catalyzed imine hydrogenation.

for this 34e dimer and the hydride ligand bridges the two ruthenium metal centers **28** (see Scheme 18) [41].

Show proposed that two ruthenium monomeric complexes are involved along the catalytic cycle resulting from the dissociation of **28** in solution (Scheme 19):

The 16e complex **29** provides **30** by activation of dihydrogen, and can also dehydrogenate a hydrogen donor [42]. This particular reactivity led Bäckvall and coworkers to use **28** as a precursor for the hydrogenation of ketones by hydrogen transfer, aerobic oxidation of alcohols and dynamic kinetic resolution of secondary alcohols [43]. Samec and Bäckvall showed that imines could be hydrogenated when using complex **28** [44,45]. In 2001, Casey et al. [46] have shown that imines are hydrogenated when using an analogue to complex **30** in which the cyclopentadienyl ligand bears two phenyl- and two tolyl substituents. Mechanistic studies and particularly deuterium isotope effects were carried out and a concerted mechanism with no coordination of the imine was proposed. Such a mechanism is equivalent to H^+ transfer from the hydroxycyclopentadienyl ligand and to H^- transfer involving the Ru-hydride bond. The two transfers are considered as simultaneous: such a net situation for aldehydes and ketones [46–48] leads to a similar picture for imines represented as **31** in Scheme 20.

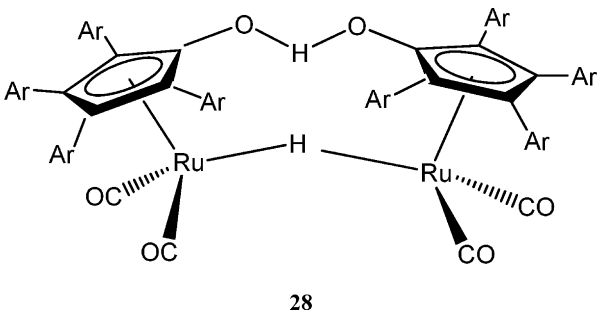

28

Scheme 18. Schematic drawing of the $[Ru_2(\mu\text{-}H)(\eta^5\text{-}C_5Ar_4OHOC_5Ar_4\text{-}\eta^5)(CO)_4]$ complex, adapted from Ref. [41].

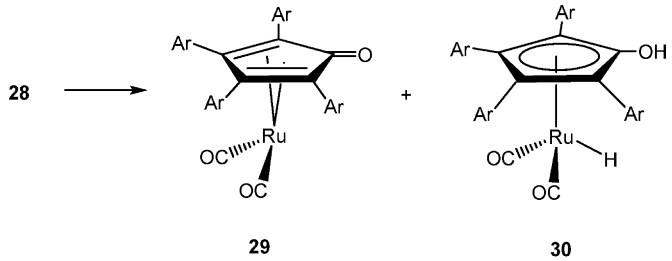

29 **30**

Scheme 19. Dissociation of complex **28** into two monomeric species, adapted from Ref. [41].

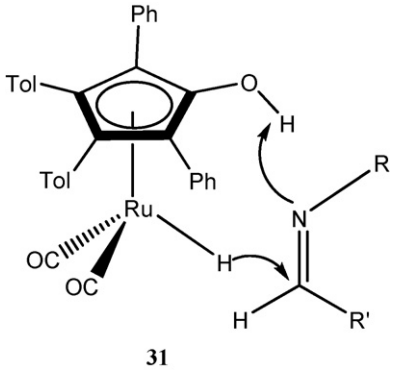

31

Scheme 20. Representation of the intermediate **31**, adapted from Ref. [48].

Complex **31** evolves towards η^4-bonded cyclopentadienone ruthenium complex **32**, with the resulting amine interacting through a hydrogen bond with the O-atom of the cyclopentadienone ligand, as shown in Scheme 21 [48]. For electron-deficient substituted imines formation of **31** is the rate-limiting step, and thus **28** and the resulting amine are observed at the end of the reaction. On the contrary, with electron-donating substituents the rate-limiting step is the coordination of the nitrogen atom to the

ruthenium center, and provides complex **32**. This kinetic behavior results in a reversible hydrogen transfer, and therefore in the imine isomerization, deuterium scrambling and moreover inverse isotopic effects [47,48].

Bäckvall and his group started also from complex **30**, for which the hydroxycyclopentadienyl ligand is bearing four phenyl substituents, and performed also mechanistic studies on the imine hydrogenation mechanism. The first intermediate initially proposed has the imine coordinated to ruthenium through the nitrogen atom, in which the two hydrogen atoms are quasi-simultaneously transferred to give the same species as **32** [49]. Recent DFT calculations complete the full mechanism and show that a first intermediate is formed in which an OH–hydrogen bond interacts between the hydroxyl substituent and the imine-nitrogen atom [50].

The two research groups demonstrate that the hydrogen transfer from the OH group and another one from the hydride require almost the same energy and are, from a kinetic point of view, quasi-simultaneous. Bäckvall et al. propose an inner-sphere mechanism, whereas Casey et al. consider an outer-sphere mechanism. Indeed, in the latter case no vacant coordination site can be created, the imine does not coordinate to ruthenium and in a concerted process the hydride ligand attacks the carbon atom of the imine group and the OH group transfers its proton to nitrogen. The resulting isolated complex is **32**. For their part, Bäckvall et al. propose that a first interaction occurs between the nitrogen atom and the hydroxyl group, before to have the nitrogen coordination and then the hydride transfer. In this case the coordination of the nitrogen atom is possible because the phenyl substituents assist the ring slippage of the cyclopentadienyl ligand from η^5- towards η^2/η^3-hapticity.

The two groups of Casey and Bäckvall have studied the isotopic effects, performed trapping experiments and made DFT calculations [48,50–54]. The electronic effects of the substituents borne by the imine induce differences in both O–H and Ru–H transfer rates. Similarly, the same electronic effects play a determinant role in the trapping of the resulting amine by coordination to ruthenium. Gas phase DFT calculations led Casey et al. to conclude that an outer sphere mechanism is occurring, whereas similar calculations carried out by Bäckvall et al. with a continuum solvent model are consistent with an inner sphere process. The main disagreement between the two proposals is related to the coordination of the imine to ruthenium, through the nitrogen atom. In fact, this coordination can occur if a vacant position is open on ruthenium by ring slippage of the substituted-Cp moiety. Bäckvall et al. have shown that this situation does occur provided solvated species are introduced in the calculations. However, Casey et al. interpret their trapping experiments of the resulting amine as an evidence of the absence of imine coordination; their results are consistent with the outer-sphere reduction to give the corresponding amine inside a solvent cage, the amine coordination proceeding more rapidly than diffusion from the solvent cage. Indeed, in a **32**-type complex including a labeled diamine, the fast isomerization process for the interaction of one or the other nitrogen atom with the cyclopentadienone would preclude any nitrogen coordination to ruthenium. Recently, Bäckvall et al. have demonstrated that there is no solvent cage effect during the reduction, which would support the outer-sphere mechanism, so that the authors are strengthened in the inner-sphere mechanism [55].

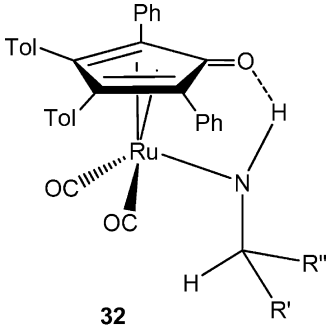

32

Scheme 21. Representation of the intermediate **32**, adapted from Ref. [48].

It is worth noting that no deep investigation has been carried out on the intimate mechanism by which the reaction of dihydrogen regenerates species **30**.

If we take into account the various substituents borne by the imine and the electronic properties and the steric hindrance they provide to the substrate, small differences result in the relative heights of the two transition states for the two hydrogen transfers. Thus, we can propose a catalytic cycle (Scheme 22) which would be consistent with the two deep studies carried out by Casey's and Bäckvall's research groups.

This catalytic cycle deserves some comments. The active species **30** lies the R-N=C(R′)(R″) imine by one hydrogen bond between the imine-nitrogen atom and the hydroxyl-hydrogen atom giving the 18e intermediate **33**. The Casey's and Bäckvall's groups consider that presumably a weak hydrogen bond is present. Species **33** evolves toward the 18e intermediate **34** in which the proton has been transferred to the nitrogen atom giving non-coordinated iminium species in a zwitterionic entity where an anionic ruthenium center coordinates the η^4-cyclopentadienone ligand. Species **34** evolves through a second ring slippage toward complex **35** whose structure has been proposed from DFT calculations carried out in solvent medium [50]: in this zwitterionic species the ruthenium metal binds the iminium C=N double bond, the coordination sphere being completed to 18e by the η^2-cyclopentadienone ligand. The fundamental 1,2-*cis*-migration step in which the hydride ligand attacks the carbon atom, and then the nitrogen atom coordinates the ruthenium center, produces the 16e species **36** in which we have maintained a η^2-coordination mode for the cyclopentadienone ligand. Thus, the catalytic cycle can be pursued by η^2-coordination of dihydrogen as usual in the ruthenium chemistry, followed by the oxidative addition reaction giving **37**. Hydride transfer to the C=C double bond of the cyclopentadienone gives presumably the intermediate **38** after isomerization through a keto-enolic process. Elimination of the amine restores the active species **30**. In a very recent theoretical analysis, Lledós et al. show that, if they take into account the solvent effects and the presence of the phenyl substituents on the hydroxycyclopentadienyl ligand, the two hydrogen transfers become asynchronous in the transition state, the proton being transferred first. A 4 kcal gain is in favor of the outer-sphere mechanism [56].

The two activation energies for the **34** → **35** and **35** → **36** steps should be relatively close and their differences should be due to the nature of various imine substituents. Thus, the catalytic cycle proposed in Scheme 22 should reconcile the two mechanisms.

2.3. Mechanism of the titanocene-catalyzed hydrogenation of imines

An interesting approach was done by Buchwald and Willoughby by using titanium(III) complexes [57,58,2,3]. Various acyclic and cyclic imines can be hydrogenated under medium to high pressures (5–170 bar), mainly in the asymmetric mode. We will analyze first the mechanism of the hydrogenation reaction before to consider its enantioselectivity.

The authors start from the Brintzinger *ansa*-diindenyldichloro (or binaphtolato) titanium(IV) complexes [4]. After removal of the chloro or binaphtolato ligands, they react them with phenylsilane

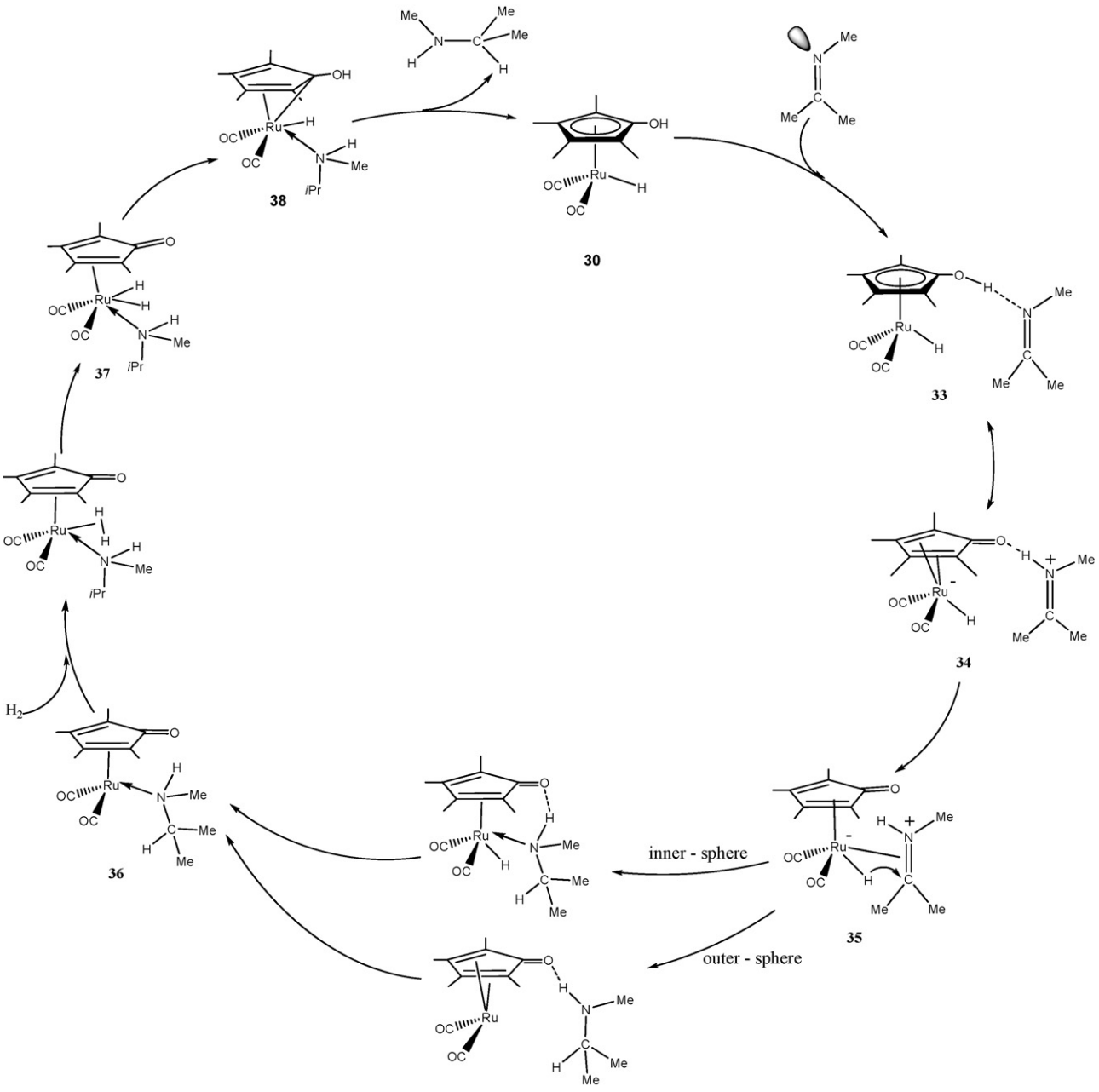

Scheme 22. Catalytic cycle based on the Casey's and Bäckvall's studies.

to end up with an active hydrogenation catalyst which is presumably a Ti(III)-hydride species of the type Cp_2TiH **39**. Coordination of the imine through the C=N bond to **39**, giving **40**, followed by the 1,2-hydride migration on the carbon atom leads to the amido-titanium(III) complex **41** (Scheme 23).

Species **41** further coordinates dihydrogen in a η^2-mode (**42**). The four-center intermediate **43**, which is classically proposed in the chemistry of early transition metals, can evolve towards complex **39** by elimination of the corresponding amine.

Concerning the asymmetric hydrogenation version, the study of Willoughby and Buchwald focused on imines bearing various substituents [57,58,2,3]. An enantiomeric excess as high as 99% can be achieved for cyclic imines, such as 2-phenylpyrroline, at 45 °C, under medium pressures ranging between 15 and 55 bar, for {substrate/catalyst} ratios of 20, by using complex **39** issued from the (*R*,*R*,*R*)-titanium(IV) complex (Scheme 24).

Concerning acyclic imines some crucial differences have been observed for the enantioselectivity which depend on the hydrogen pressure, and to a less extent on the solvent. The hydrogenation of N-(1-cyclohexylethylidene)benzylamine is representative of this behavior (Scheme 25) since the e.e. is reduced to 81%.

Reactivity studies have shown that the imine is hydrogenated in a relatively fast step by a 1,2-hydride-migration reaction; then a slow hydrogenolysis step operates to regenerate **39** and to produce the chiral amine. Kinetic studies have evidenced the formation of an aldimine in few amounts arising from an isomerization reaction involving a β-H elimination process after the first hydride transfer. In addition, a slow interconversion occurs between the two *syn*- and *anti*-isomers of the starting acyclic imine, and the syn-isomer coordinates faster to the hydride-titanium active species. These two cumulative effects play a significant role in the reaction performances.

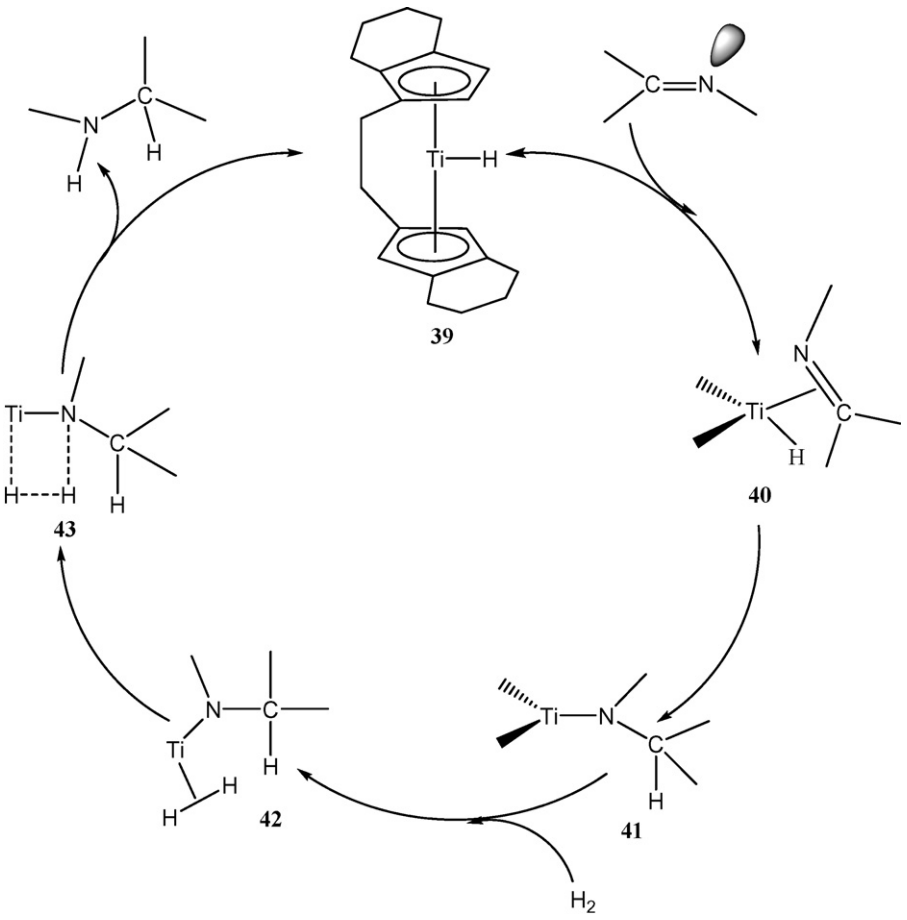

Scheme 23. Catalytic cycle for the hydrogenation of imines by titanium, adapted from Ref. [3].

The β-H elimination, which involves a hydrogen atom on one of the two α-carbon atoms bonded to the nitrogen atom and produces the aldimine or back the imine, is consistent with the η^2-coordination of the C=N double bond onto the titanium center (**40**). Willoughby and Buchwald transpose the model calculated by Lauher and Hoffmann [59] for the coordination of an alkene ligand on d^0, d^1 or d^2 metal centers to propose the intermediate **40** and its further reaction to give species **41** by 1,2-*cis*-migration of the hydride ligand onto the coordinated imine. In species **40** the imine ligand would probably not be coordinated by the nitrogen lone pair, because the carbon atom, non-bonded to titanium, would not be enough electrophilic to be attacked by the hydride ligand.

This C=N coordination explains also the enantiofacial discrimination for the approach of the imine, and rationalization of the origin of the enantioselectivity has been done. In fact, the substituent on the nitrogen atom appears to play the main role in the steric interactions with the tetrahydroindenyl ligand. The *anti*-imine is shown to coordinate titanium in such a way that the (R)-amine is produced. Similarly, on the same (*R*,*R*,*R*)-**39** complex the *syn*-imine isomer leads to the expected (S)-amine. In addition to the size of the nitrogen-substituent, the presence of significantly large groups on the carbon atom plays a secondary role in promoting this enantioselectivity.

The mechanism of the hydrogenolysis step has not been explored in details since the authors focused their studies on the determining steps governing the enantioselectivity. To the best of our knowledge, no further investigations have been carried out.

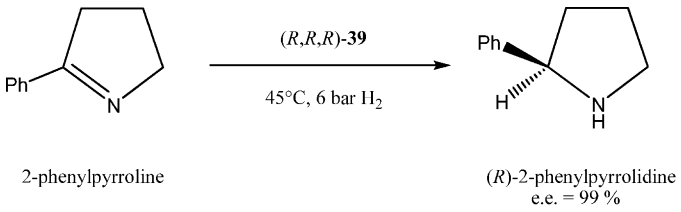

Scheme 24. Hydrogenation of 2-phenylpyrroline by species **39**, adapted from Ref. [3].

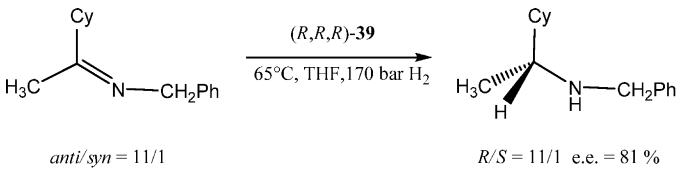

Scheme 25. Hydrogenation of N-(1-cyclohexylethylidene)benzylamine, adapted from Ref. [3].

2.4. Miscellaneous metal-catalyzed asymmetric hydrogenations

A few palladium precursors have been tested in the hydrogenation of imines. Starting from bis(trifluoroacetato)palladium and adding (*R*)-BINAP in fluoroalcohol medium, various fluorinated iminoesters have been hydrogenated at 100 bar and room temperature [60,61]. Good yields, ranging from 70 to 99% can be reached, and e.e.'s up to 91% in trifluoroethanol have been obtained. The exact role of the fluorinated solvent remains to be elucidated.

More recently, N-tosylimines have been successfully hydrogenated by electron-donating rigid diphosphines, especially the (*S*,*S*,*R*,*R*)-TangPhos ligand in which the two phosphorus atoms are chiral [62]. The cationic rhodium complexes, produced by addition of one equivalent of the diphosphine ligand to the bis(η^4-cyclooctadiene) precursor [Rh(COD)$_2$][BF$_4$], are characterized by good conversions and e.e.'s ranging from 61 to 94%. Moreover, among several palladium complexes, the Pd(OCOCF$_3$)$_2$/TangPhos system, under 75 bar H_2 pressure and at 40 °C, for 12 h, with S/C = 100, gives rise to the most satisfactory results: 99% conversion of (N-tosyl)(methylbenzyl)imine and 99% e.e. In these N-tosylimines the phenyl group can be replaced by various aryl and even alkyl substituents, and except for a cyclopropyl group-containing substrate, high e.e.'s are still attained.

The weakly coordinating trifluoroacetato anion appears to play a significant role in this palladium system, provided H_2 high pressures are maintained. Although this latter catalytic system seems to be attractive, no mechanism has been proposed yet to have a clear understanding of the role played by the electron-withdrawing tosyl group and the trifluoroacetato ligand.

3. Enamides

It seemed to us of interest to extend the analysis of the hydrogenation mechanism of imines to that of functionalized prochiral enamines, especially N-acylenamines, since many studies have been devoted to the mechanistic aspects which govern the enantioselectivity of this reaction.

Prochiral acetamidoesters have been studied as early as in the 1970s and many cationic rhodium complexes containing diphosphine ligands have been investigated. Most of the leading works on the mechanism of these substrates are due to the pioneering studies carried out by Brown and Halpern and their research groups [63–69].

Preliminary studies on non-chiral diphosphine ligands led Halpern [65] to identify that the active species is a cationic rhodium(I), [Rh(diphos)(solvent)$_2$]$^+$ complex **44**, in which the acetamidoester substitutes the two solvato ligands, the solvent being methanol, and coordinates the metal centre in a chelating mode, both by the carbon–carbon double bond and the oxygen atom of the acetamido function but not by the ester oxygen atom (complex **45**). This step was considered the only one being reversible in the catalytic cycle. As shown in Scheme 26 where the main steps of catalysis are displayed, the activation of dihydrogen, giving **46**, is followed by the first hydride transfer onto the terminal β-carbon atom producing a benzyl group and the simultaneous bonding of the chirogenic α-carbon atom to the metal centre (species **47**). Then, reductive elimination occurs to produce the corresponding amine and restore the active species **44** in its di-solvated form.

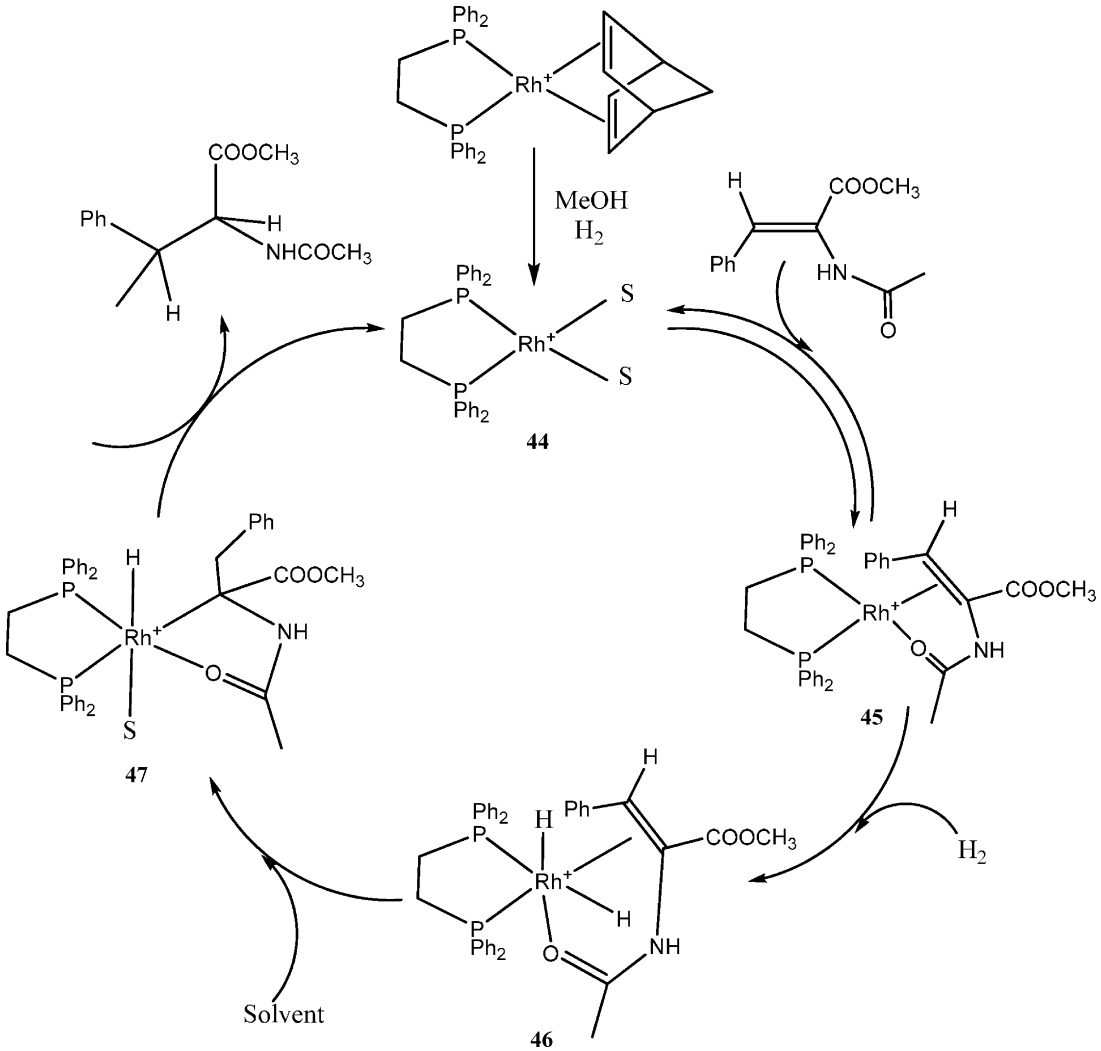

Scheme 26. Catalytic cycle of the hydrogenation of an enamide, adapted from Ref. [65].

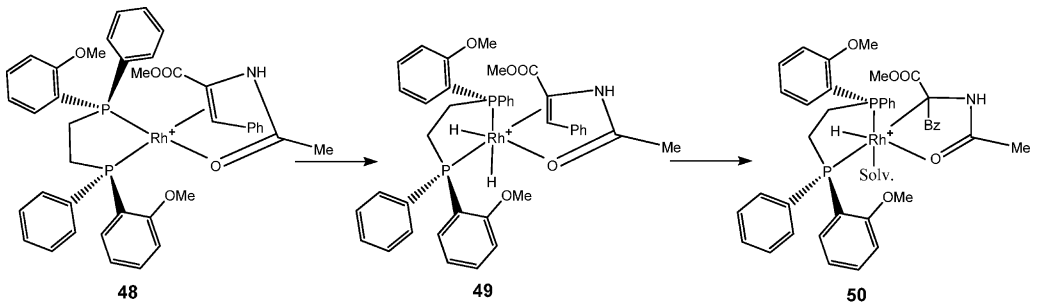

Scheme 27. Chiral intermediates, adapted from Ref. [69].

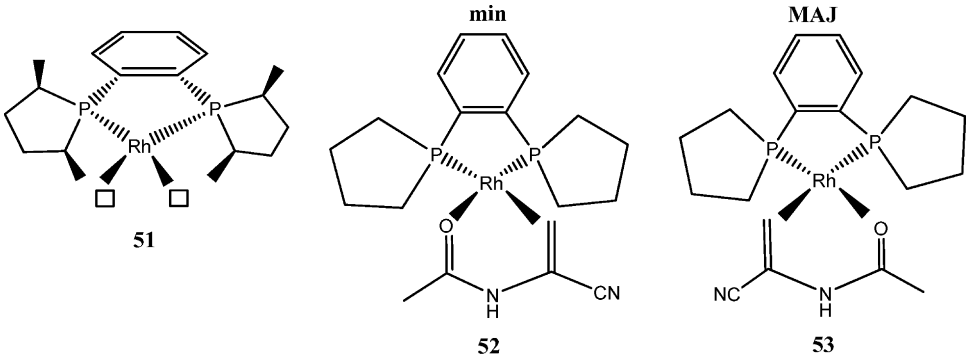

Scheme 28. Representation of species **46**, and the two **min** (**52**) and **MAJ** (**53**) diastereomers resulting from the coordination of the enamide substrate, adapted from Ref. [70].

Further introduction of a chiral diphosphine ligand led Landis and Halpern [69] to investigate in depth the step where the enantioselectivity does occur. Their analysis showed that coordination of the substrate to the rhodium centre proceeds both through the approach of the enantiotopic face of the C=C double bond and the coordination of the acetamido group, such a process precluding the decoordination–rotation–recoordination of the C=C double bond. Scheme 27 presents this coordination as well as the formation of the dihydride species and then the alkyl chiral species according to the Landis and Halpern studies [69].

In 2000, Landis and Felgus performed computational calculations, some of them at high level of theory. Thus, they confirmed the unsaturated mechanism in which the [Rh(diphos*)(acetamido)]$^+$ **48** complex is produced first, giving then a more precise insight onto the key intermediates [70,71]. Calculations are fully consistent with several crystal structures on related square planar complexes containing chiral diphosphine ligands, NMR studies and kinetic measurements [64,72,73]. In these calculations the (*R*,*R*)-Me-DuPHOS ligand was entirely taken in account especially with the four CH_3 groups, whereas the model enamide substrate was chosen as α-formamidoacrylonitrile. The [RhP^*_2] core, **51**, is displayed in Scheme 28 with two squares indicating the two vacant positions which will be occupied after coordination by the C=C double bond and the formamide-oxygen atom, either the *re* or the *si* face of the alkene approaching the rhodium atom, and giving the first enantioselection to provide **52** and **53**, respectively.

Just after the chelation of the substrate, the next step, which is rate-determining, concerns the approach of dihydrogen followed by its oxidative addition producing a dihydride-species similar to **49**. The [Rh(P^*_2)(formamidoacrylonitrile)(η^2-H_2)]$^+$ intermediate adopts a trigonal bipyramidal geometry, and in the more stable isomers, the equatorial plane contains the η^2-H_2 ligand, the C=C double bond and one phosphorus atom, whereas the oxygen atom lies in an axial position trans to the second phosphorus atom. Thus among the eight possible diastereomers resulting from the H_2 approach up or down the rhodium square-plane, along the P–Rh–O or the P–Rh–alkene directions, only two six-coordinate isomers are the most stable after the oxidative addition.

Coordination of either the *re* face or the *si* face of the enamide produces the two **MAJ** (**53**) and **min** (**52**) species (MAJOR and minor according to the nomenclature of Landis and Halpern [69]) with a difference of free energy of 4.4 kcal mol^{-1}, corresponding roughly to 99% of the first isomer and 1% of the second. Thus, two parallel pathways are followed during catalysis, the {**MAJ** + H_2} system being the zero energy level.

For the **MAJ** isomer the α-carbon atom of the double bond is very close to the coordination plane for electronic reasons, whereas in the **min** isomer the β-carbon lies nearly this plane. However, when the H_2 molecule approaches the rhodium center in the **MAJ** isomer the C=C double bond must rotate significantly so that the

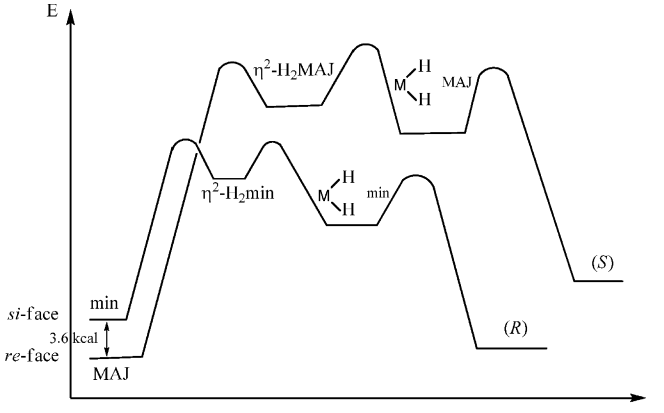

Scheme 29. Simplified free energy diagram displaying the higher reactivity of the min-isomer, adapted from Refs. [70,71].

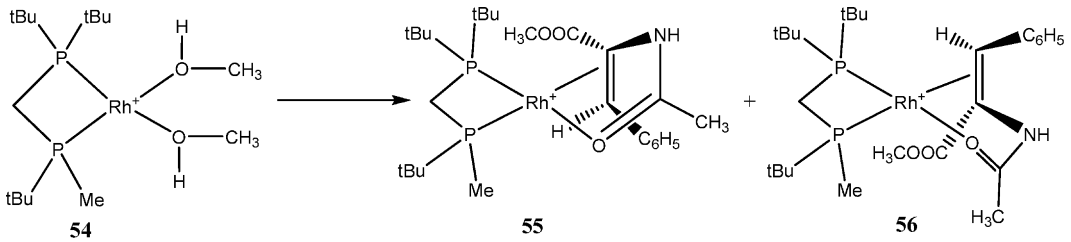

Scheme 30. The two kinetics isomers resulting from the coordination of acetamidocinnamate, adapted from Ref. [75].

electronic benefit is lost and the amido group comes into a hindered quadrant. On the contrary, for the **min** isomer, the distortion is less pronounced and the amido group is then placed in an unhindered quadrant. Thus, the reactivity of the **min**-isomer is largely favored and explains why it is responsible for the 99% enantioselectivity of the hydrogenation reaction (Scheme 29).

Very recent studies carried out by Imamoto and coworkers [74,75] allow to have a deeper insight onto the mechanism of the reaction of H_2 with the [(diphos*)Rh(substrate)]$^+$ intermediates taking into account the crucial role of the solvent. Indeed, starting from the chiral diphosphine ligand (t-Bu)$_2$PCH$_2$P*(CH$_3$)(t-Bu) which presents a constrained bridge between the two non-equivalent phosphorus atoms, low temperature NMR studies and theoretical calculations of the methanol-solvated species shed light on the intramolecular isomerization process between the two *R* and *S*-(α)-acetamidocinnamate complexes to provide an enantiomer with 97% e.e. At −100 °C the precursor [Rh(1,5-η^4-C$_8$H$_{12}$){(t-Bu)$_2$PCH$_2$P*(CH$_3$)(t-Bu)}]$^+$ reacts in methanol with dihydrogen to produce cyclooctane and [Rh{(t-Bu)$_2$PCH$_2$P*(CH$_3$)(t-Bu)}(MeOH)$_2$] **54** (Scheme 30). Then, under argon atmosphere the substrate reacts to give the two kinetic isomers in which the C=C double bond is coordinated from the side of the non-chiral phosphorus atom, (t-Bu)$_2$P, the oxygen-acetamido atom being coordinated in the fourth position of the square plane (Scheme 30, diastereomers **55** and **56**).

Above −80 °C a slow rearrangement occurs during which the C=C double bond coordinates from the side of the stereogenic phosphorus ligand, the oxygen-acetamido atom being coordinated along all the process (Scheme 31, species **57**). NMR observations carried out at −80 °C in methanol show that the complex in which one solvent molecule is hydrogen-bonded to the ester oxygen atom of the substrate coordinated in a chelate mode (**58**) does not react directly with dihydrogen. In fact, this complex is in a slow equilibrium with an intermediate species containing one methanol molecule bonded to rhodium through the oxygen atom and hydrogen-bonded to the oxygen atom of the ester group of the decoordinated C=C double bond (intermediate **59**). It reacts very quickly with H_2 to provide the dihydrogenated product. DFT calculations confirmed this unexpected pathway and gave validation that the recoordination of the double bond provides the right octa-

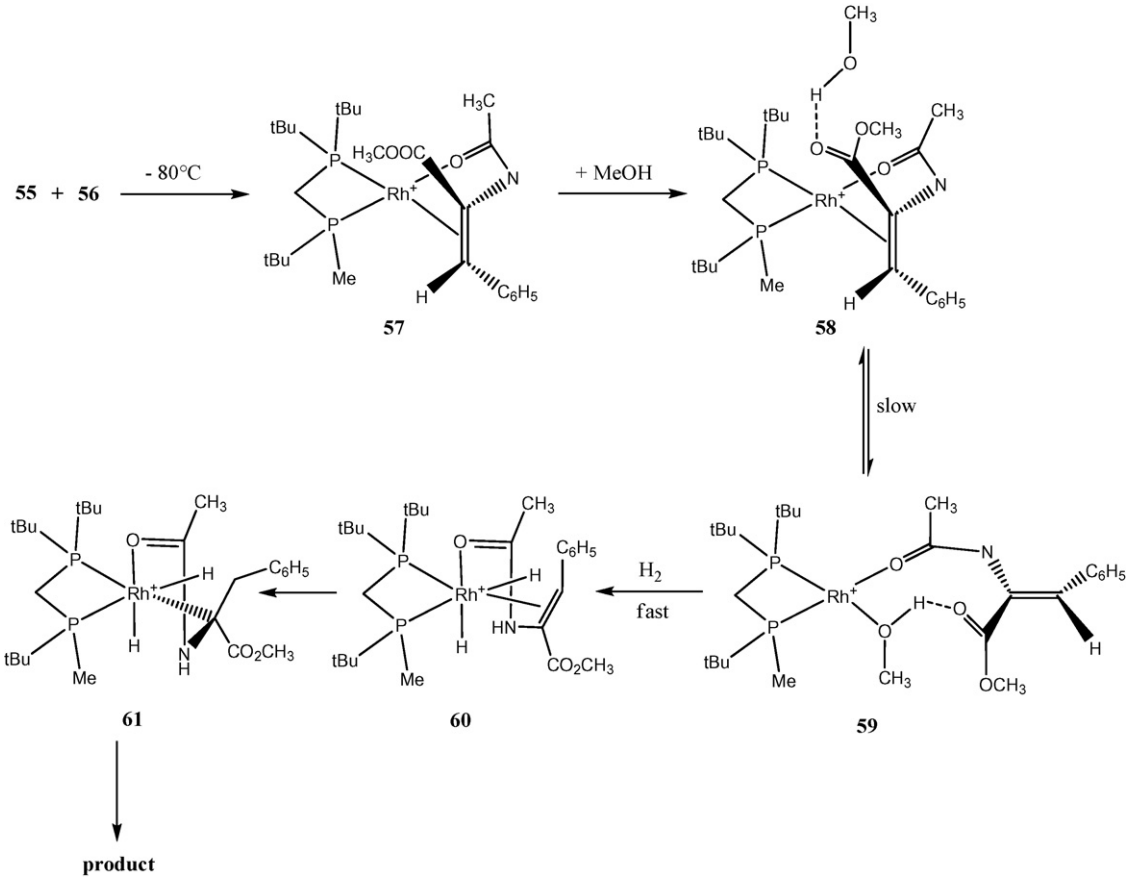

Scheme 31. Reaction pathway giving the (S)-isomer, adapted from Ref. [75].

hedral stereoisomer **60** which precedes the irreversible migratory insertion step giving species **61** (Scheme 31).

Moreover, using complexes containing the diphosphine ligands where the two phosphorus centers are chirogenic, Imamoto et al. showed that the stereodifferentiation stems from the privileged approach of one enantiotopic face of the double bond to minimize the steric interaction between the phosphorus substituents and the substrate [74].

However, Imamoto and Gridnev [76] carried out mechanistic NMR studies at very low temperature (−100 °C) with several different chiral ligands. They identified that a second pathway could exist in which the active species reacts first with dihydrogen to provide the dihydride $[Rh(H)_2(diphos^*)(solv)_2]^+$ intermediate.

The first and this latter pathway have been called the *unsaturated* and the *hydride* ones. Depending on the basicity of the ligand, experimental evidences and DFT theoretical computations have shown that two alternative pathways can compete. The corresponding intermediates have been isolated, characterized by NMR, and their geometry and energy calculated. Electron-donating groups carried by the phosphorus atoms increase the electron density on the rhodium atom and thus privilege the *dihydride* pathway. Thus, the oxidative addition of dihydrogen occurs in the early stage to provide the $[Rh(H)_2(diphos^*)(solv)_2]^+$ species to which the substrate will then coordinate.

Whatever the *unsaturated* or the *dihydride* pathway is followed, the same $[Rh(H)_2(diphos^*)(substrate)]^+$ complex is formed for which the eight diastereoisomers are expected. Among these eight unstable species, computational studies showed that only two present lower energetic barrier in each mechanism and could explain the observed enantioselection. However, reversible equilibria exist between all these species whatever is the pathway, and the enantioselection occurs when the equatorial hydride ligand is transferred to the C_β carbon atom in the migratory insertion step giving a monohydride rhodium–chiral carbon bond species, as shown in Scheme 31 (species **61**).

In addition, in the diastereoisomeric dihydride complexes in which the oxygen is in an axial position and the double bond in an equatorial position, Imamoto et al. reported that one hydride is axial whereas the second one is equatorial, and established by isotopic studies, mainly involving HD, that the equatorial hydride is transferred to the C_β carbon atom. This is the irreversible stereodetermining step in which a hexacoordinated solvated monohydride species results containing the chiral carbon atom bound to rhodium. The last step is then the reductive elimination providing the chiral amine and the active species [77].

4. Conclusion

The synthesis of precursors of chiral amines by coordination catalysis is still nowadays a subject of great importance and a deep understanding of the mechanisms that govern the enantioselectivity is essential for obtaining efficient catalysts. In the early stage, Brown and then, Landis and Halpern developed pioneering investigations on the hydrogenation of enamides showing that the chelating effect of the substrate assists significantly the asymmetric induction. DFT calculations provided a powerful complement to the low temperatures NMR studies to intercept relevant intermediates in the catalytic cycle. The two pathways which involve the coordination of the enamide to the cationic $[Rh(diphos^*)]^+$ entity or the oxidative addition of dihydrogen on it, are in competition before the first irreversible hydride transfer occurs, providing a chiral alkyl group bound to rhodium.

Concerning imines, the catalytic hydrogenation involves mainly rhodium, iridium, ruthenium, and to a lesser extent titanium. The mechanisms involving rhodium and iridium complexes remain of a great complexity, and recent contribution by Claver and Fernandez [78] shows that this subject is still investigated. Analysis of these mechanisms led us to propose that they should involve the formation of an iminium key intermediate. Concerning the main mechanism on the ruthenium catalyzed-hydrogenation, in the peculiar case of the Shvo's complex, simultaneous transfers of a proton and a hydride occur. The most recent calculations [55,56] demonstrate that, when the solvent is taken into account, these two transfers are no more synchronous. With regard to the two inner- or outer-sphere mechanisms described in the literature, we propose that these two very fast steps involve firstly a proton transfer to produce an iminium species and secondly its coordination to the ruthenium center, before the *cis*-migration of the hydride ligand occurs.

However, regarding enamine substrates, besides titanium and its mechanism investigated, there are few efficient catalytic systems. Recent satisfactory results for producing chiral amines through hydrogenation of substituted enamines are encouraging [15,18].

Although an important library of chiral ligands exists involving not only the traditional diphosphines, but also mixed ligands containing a phosphorus coordinating atom associated with a nitrogen atom, or a carbene donating center, a correct adjustment of the coordination sphere is necessary to maintain simultaneously reactivity, productivity and enantioselectivity.

At the present time the analytical tools to obtain IR, Raman, NMR informations under pressure, in the conditions of catalysis, could contribute highly to design coordination precursors including appropriate ligands. In addition, modern DFT calculations provide complementary information on the intermediate species that allow validating the most probable catalytic pathway since the relative energies of all the intermediates which have been intercepted or imagined, even from kinetic studies, can be calculated with good confidence.

References

[1] E.N. Jacobsen, A. Pfaltz, H. Yamamoto (Eds.), Comprehensive Asymmetric Catalysis, Springer-Verlag, Berlin, Heidelberg, 1999.
[2] C.A. Willoughby, S.L. Buchwald, J. Am. Chem. Soc. 116 (1994) 8952.
[3] C.A. Willoughby, S.L. Buchwald, J. Am. Chem. Soc. 116 (1994) 11703.
[4] F.R.W.P. Wild, J. Zsolnai, G. Huttner, H.H. Brintzinger, J. Organomet. Chem. 232 (1982) 233.
[5] I. Ojima (Ed.), Catalytic Asymmetric Synthesis, second edition, Wiley–VCH, New York, 2000.
[6] F. Agbossou-Niedercorn, in: B. Cornils, W.A. Herrmann (Eds.), Applied Homogeneous Catalysis with Organometallic Compounds, second edition, Wiley–VCH, Weinheim, 2002, p. 1014.
[7] W. Tang, X. Zhang, Chem. Rev. 103 (2003) 3029.
[8] G. Erre, S. Enthaler, K. Junge, S. Gladiali, M. Beller, Coord. Chem. Rev. 252 (2008) 471.
[9] A. Grabulosa, J. Granell, G. Muller, Coord. Chem. Rev. 251 (2007) 25.
[10] M.C. Perry, K. Burgess, Tetrahedron: Asymm. 14 (2003) 951.
[11] D. Baskakov, W.A. Herrmann, E. Herdtweck, S.D. Hoffmann, Organometallics 26 (2007) 626, and references quoted.
[12] F. Spindler, H.-U. Blaser, in: J.G. de Vries, C.J. Elsevier (Eds.), Handbook of Homogeneous Hydrogenation, Wiley–VCH, 2007, p. 1193.
[13] N. Lee, S.L. Buchwald, J. Am. Chem. Soc. 116 (1994) 5985.
[14] P. Cheruku, T.L. Church, A. Trifonova, T. Wartmann, P.G. Andersson, Tetrahedron Lett. 49 (2008) 7290, and references quoted.
[15] G.-H. Hou, J.-H. Xie, P.-C. Yan, Q.-L. Zhou, J. Am. Chem. Soc. 131 (2009) 1366, and references quoted.
[16] A. Baeza, A. Pfaltz, Chem. Eur. J. 15 (2009) 2266, and references quoted.
[17] V.I. Tararov, T.H. Riemeier, J. Holz, A. Börner, Tetrahedron Lett. 41 (2000) 2351.
[18] G.H. Hou, J.H. Xie, L.X. Wang, Q.L. Zhou, J. Am. Chem. Soc. 128 (2006) 11774.
[19] H. Brunner, in: B. Cornils, W.A. Herrman (Eds.), Applied Homogenous Catalysis with Organometallic Compounds, second edition, Wiley–VCH, Weinheim, 2002, p. 195.
[20] R. Noyori, Angew. Chem. Int. Ed. 41 (2002) 2008.
[21] W.S. Knowles, Angew. Chem. Int. Ed. 41 (2002) 1998.
[22] A. Levi, G. Modena, G. Scorrano, J. Chem. Soc. Chem. Commun. (1975) 6.
[23] A.J. Blacker, in: J.G. de Vries, C.J. Elsevier (Eds.), Handbook of Homogeneous Hydrogenation, Wiley–VCH, 2007, p. 1215.
[24] P. Marcazzan, B.O. Patrick, B.R. James, Organometallics 22 (2003) 1177.
[25] P. Marcazzan, B.O. Patrick, B.R. James, Russ. Chem. Bull., Int. Ed. 52 (2003) 2715.

[26] M.B. Ezhova, B.O. Patrick, B.R. James, M.E. Ford, F.J. Waller, Russ. Chem. Bull., Int. Ed. 52 (2003) 2707.
[27] P. Marcazzan, C. Abu-Gnim, K.N. Seneviratne, B.R. James, Inorg. Chem. 43 (2004) 4820.
[28] M.B. Ezhova, B.O. Patrick, B.R. James, M.E. Ford, J. Mol. Catal. 224 (2004) 71.
[29] P. Marcazzan, B.O. Patrick, B.R. James, Inorg. Chem. 43 (2004) 6838.
[30] M.B. Ezhova, B.O. Patrick, K.N. Seneviratne, B.R. James, F.J. Waller, M.E. Ford, Inorg. Chem. 44 (2005) 1482.
[31] P. Marcazzan, B.O. Patrick, B.R. James, Organometallics 24 (2005) 1445.
[32] M.B. Ezhova, B.O. Patrick, B.R. James, Organometallics 24 (2005) 3753.
[33] P. Marcazzan, B.O. Patrick, B.R. James, J. Mol. Catal. 257 (2006) 26.
[34] P. Barbaro, C. Bianchini, A. Meli, M. Moreno, F. Vizza, Organometallics 21 (2002) 1430.
[35] V.R. Landaeta, B.K. Muñoz, M. Peruzzini, V. Merrera, C. Bianchini, R.A. Sanchez-Delgado, Organometallics 25 (2006) 403.
[36] F. Torres, E. Sola, M. Martin, J.A. López, F.J. Lahoz, L.A. Oro, J. Am. Chem. Soc. 121 (1999) 10632.
[37] F. Torres, E. Sola, M. Martin, C. Ochs, G. Picazo, J.A. López, F.J. Lahoz, L.A. Oro, Organometallics 20 (2001) 2716.
[38] M. Martin, E. Sola, S. Tejero, J.L. Andrés, L.A. Oro, Chem. Eur. J. 12 (2006) 4043.
[39] M. Martin, E. Sola, S. Tejero, J.A. López, L.A. Oro, Chem. Eur. J. 12 (2006) 4057.
[40] Y. Blum, D. Czarkie, Y. Rahamim, Y. Shvo, Organometallics 4 (1985) 1459.
[41] Y. Shvo, D. Czarkie, Y. Rahamim, J. Am. Chem. Soc. 108 (1986) 7400.
[42] B. Schneider, I. Goldberg, D. Reshef, Z. Stein, Y. Shvo, J. Organomet. Chem. 588 (1999) 92.
[43] J.S.M. Samec, J.-E. Bäckvall, P.G. Andersson, P. Brandt, Chem. Soc. Rev. 35 (2006) 237.
[44] J.S.M. Samec, J.-E. Bäckvall, Chem. Eur. J. 13 (2002) 2955.
[45] J.S.M. Samec, L. Mony, J.-E. Bäckvall, Can. J. Chem. 83 (2005) 909.
[46] C.P. Casey, S.W. Singer, D.R. Powell, R.K. Hayashi, M. Kavana, J. Am. Chem. Soc. 123 (2001) 1090.
[47] C.P. Casey, J.B. Johnson, J. Org. Chem. 68 (2003) 1998.
[48] C.P. Casey, J.B. Johnson, J. Am. Chem. Soc. 127 (2005) 1883.
[49] J.S.M. Samec, A.H. Éll, J.-E. Bäckvall, Chem. Commun. (2004) 2748.
[50] T. Privalov, J.S.M. Samec, J.-E. Bäckvall, Organometallics 26 (2007) 2840.
[51] C.P. Casey, J.B. Johnson, Can. J. Chem. 83 (2005) 1339.
[52] J.S.M. Samec, A.H. Éll, J.B. Åberg, T. Privalov, L. Eriksson, J.-E. Bäckvall, J. Am. Chem. Soc. 128 (2006) 14293.
[53] C.P. Casey, G.A. Bikzhanova, Q. Cui, I.A. Guzei, J. Am. Chem. Soc. 127 (2005) 14062.
[54] C.P. Casey, T.B. Clark, I.A. Guzei, J. Am. Chem. Soc. 129 (2007) 11821.
[55] J.B. Åberg, J.-E. Bäckvall, Chem. Eur. J. 14 (2008) 9169.
[56] A. Comas-Vives, G. Ujaque, A. Lledós, Organometallics 27 (2008) 4854.
[57] C.A. Willoughby, S.L. Buchwald, J. Am. Chem. Soc. 114 (1992) 7562.
[58] C.A. Willoughby, S.L. Buchwald, J. Org. Chem. 58 (1993) 7627.
[59] J.W. Laucher, R. Hoffman, J. Am. Chem. Soc. 98 (1976) 1729.
[60] H. Abe, H. Amii, K. Uneyama, Org. Lett. 3 (2001) 313.
[61] A. Suzuki, M. Mac, H. Amii, K. Uneyama, J. Org. Chem. 69 (2004) 5132.
[62] Q. Yang, G. Shang, W. Gao, J. Deng, X. Zhang, Angew. Chem. Int. Ed. 45 (2006) 3832.
[63] J. Halpern, D.P. Riley, A.S.C. Chan, J.J. Pluth, J. Am. Chem. Soc. 99 (1977) 8055.
[64] A.S.C. Chan, J.J. Pluth, J. Halpern, Inorg. Chim. Acta 37 (1979) L477.
[65] A.S.C. Chan, J. Halpern, J. Am. Chem. Soc. 102 (1980) 838.
[66] J.M. Brown, D. Parker, Organometallics 1 (1982) 950.
[67] J.M. Brown, L.R. Canning, A.J. Downs, A.M. Forster, J. Organomet. Chem. 255 (1983) 103.
[68] J.M. Brown, P.J. Maddox, J. Chem. Soc. Chem. Commun. (1987) 1276.
[69] C.R. Landis, J. Halpern, J. Am. Chem. Soc. 109 (1987) 1746.
[70] S. Felgus, C.R. Landis, J. Am. Chem. Soc. 122 (2000) 12714.
[71] C.R. Landis, S. Felgus, Angew. Chem. Int. Ed. 39 (2000) 2863.
[72] A.S.C. Chan, J.J. Pluth, J. Halpern, J. Am. Chem. Soc. 102 (1980) 5952.
[73] B. McCulloch, J. Halpern, M.R. Thompson, C.R. Landis, Organometallics 9 (1990) 1392.
[74] I.D. Gridnev, T. Imamoto, Acc. Chem. Res. 37 (2004) 633.
[75] I.D. Gridnev, T. Imamoto, G. Hoge, M. Kouchi, H. Takahashi, J. Am. Chem. Soc. 130 (2008) 2560.
[76] I.D. Gridnev, M. Yasutake, N. Higashi, T. Imamoto, J. Am. Chem. Soc. 123 (2001) 5268.
[77] T. Imamoto, T. Itoh, K. Yoshida, I.D. Griednev, Chem. Asian J. 3 (2008) 1636.
[78] C. Claver, E. Fernandez, in: P.G. Andersson, I.J. Munslow (Eds.), Modern Reduction Methods, Wiley–VCH, Verlag, Weinheim, 2008, p. 237.